Phase diagram of the frustrated spatially-anisotropic $S=1$ antiferromagnet on a square lattice

H. C. Jiang,[1] F. Krüger,[2] J. E. Moore,[3] D. N. Sheng,[4] J. Zaanen,[5] and Z. Y. Weng[1]
[1]*Center for Advanced Study, Tsinghua University, Beijing 100084, China*
[2]*Department of Physics, University of Illinois, 1110 W. Green St., Urbana, Illinois 61801, USA*
[3]*Department of Physics, University of California, Berkeley, California 94720, USA*
[4]*Department of Physics and Astronomy, California State University, Northridge, California 91330, USA*
[5]*Instituut-Lorentz, Universiteit Leiden, P.O. Box 9506, 2300 RA Leiden, The Netherlands*
(Received 20 January 2009; revised manuscript received 17 April 2009; published 7 May 2009)

We study the $S=1$ square lattice Heisenberg antiferromagnet with spatially anisotropic nearest-neighbor couplings J_{1x} and J_{1y} frustrated by a next-nearest-neighbor coupling J_2 numerically using the density-matrix renormalization-group (DMRG) method and analytically employing the Schwinger-Boson mean-field theory (SBMFT). Up to relatively strong values of the anisotropy, within both methods we find quantum fluctuations to stabilize the Néel-ordered state above the classically stable region. Whereas SBMFT suggests a fluctuation-induced first-order transition between the Néel state and a stripe antiferromagnet for $1/3 \leq J_{1x}/J_{1y} \leq 1$ and an intermediate paramagnetic region opening only for very strong anisotropy, the DMRG results clearly demonstrate that the two magnetically ordered phases are separated by a quantum-disordered region for all values of the anisotropy with the remarkable implication that the quantum paramagnetic phase of the spatially isotropic J_1-J_2 model is continuously connected to the limit of decoupled Haldane spin chains. Our findings indicate that for $S=1$ quantum fluctuations in strongly frustrated antiferromagnets are crucial and not correctly treated on the semiclassical level.

DOI: 10.1103/PhysRevB.79.174409 PACS number(s): 75.50.Ee, 75.10.Jm, 75.30.Kz

I. INTRODUCTION

A striking commonality between the recently discovered iron pnictides superconductors[1–5] and the high-T_c cuprates is that in both cases superconductivity emerges on doping antiferromagnetic parent compounds. In trying to unravel the mechanisms of superconductivity frustrated quantum antiferromagnets on the square lattice have been subject to intense research over the last decades with particular interest in the extreme quantum limit $S=\frac{1}{2}$ relevant for the cuprates, whereas the interest in higher spin values increased tremendously with the discovery of the pnictides.

Thereby, the Heisenberg model with antiferromagnetic exchange couplings J_1 and J_2 between nearest neighbor (NN) and next-nearest neighbor (NNN) has served as a prototype model for studying magnetic frustration. On a classical level, one finds Néel order to be stable for $J_2/J_1 \leq 1/2$, whereas for larger ratios the classical ground state is give by a stripe-antiferromagnet with ordering wave vector $(\pi,0)$. Not surprisingly, the J_1-J_2 model has been used to rationalize the $(\pi,0)$ magnetism[6] of the iron pnictide superconductors and to subsequently calculate the magnetic excitation spectra[7,8] where the incorporation of a strong anisotropy between the NN couplings turned out to be necessary to reproduce the low-energy spin-wave excitations. Recently, it has been suggested that the strong anisotropies in the magnetism[8] but also in electronic properties[9] of the pnictides originate in the coupling to orbital degrees of freedom arising from an orbital degeneracy of an intermediate $S=1$ spin state.[10] Even if the charge degrees of freedom are not completely localized, the J_1-J_2 model can be used as the starting point for a symmetry-based analysis of magnetism and superconductivity in the iron-based superconductors.[11,12]

The $1/S$ expansion serves as a natural starting point to investigate the stability of the classical orders against quantum fluctuations which are expected to induce a paramagnetic phase near $J_2/J_1=1/2$ where both orders compete. Indeed, on the level of lowest-order linear spin-wave theory one finds an intermediate paramagnetic phase for all spin values.[13] However, the incorporation of spin-wave interactions within a modified spin-wave theory (MSWT) (Refs. 14 and 15) or the Schwinger-Boson mean-field theory (SBMFT) (Ref. 16) drastically changes this picture. Within both approaches one finds a dramatic stabilization of the classical orders by quantum fluctuation for the Néel order even up to values considerably larger than the classical threshold value $J_2/J_1=1/2$. This has been interpreted as an order-out-of-disorder phenomenon giving rise to a fluctuation induced first-order transition between the two orders. This picture has been confirmed recently by a functional one-loop renormalization-group analysis[17] where it was shown that the Néel phase becomes unstable towards a fluctuation induced first-order transition for $S>0.68$.

Surely, it is questionable if the semiclassical treatment can correctly account for the quantum fluctuations in the regime of strong frustration and small spins. In fact, in the case $S=\frac{1}{2}$ various numerical studies including exact diagonalization,[18–21] variational Monte Carlo[22,23] series expansion[24–28] as well as the coupled cluster approach[29] give the consistent picture that in the regime $0.4 \lesssim J_2/J_1 \lesssim 0.6$ no magnetic order is present clearly indicating that the aforementioned semiclassical treatments overestimate the stability of the ordered states. Another key observation of the series expansion and in particular of the unbiased exact diagonalization studies is that in the paramagnetic phase the lattice symmetry is spontaneously broken due to the formation of columnar valence-bond solid order. Such states have been predicted before[30,31] on the basis of a large N treatment for nonfrustrated systems in the absence of long-range antiferro-

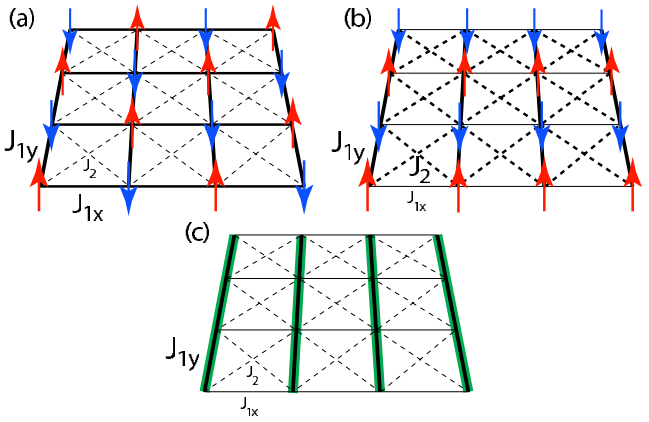

FIG. 1. (Color online) The model studied in this paper consists of a $S=1$ Heisenberg system with spatially anisotropic nearest-neighbor couplings J_{1x} and J_{1y} and isotropic next-nearest-neighbor couplings J_2. Pending the balance of these couplings one finds either a simple (a) staggered or (b) "stripe" antiferromagnetic order. In the limit of isolated chains a (c) stack of isolated Haldane spin chains is formed and based on our DMRG calculations we could conclude that these survive all the way to the isotropic limit in the vicinity of the point of maximal frustration ($J_2/J_1=0.5$).

magnetic order. These depend however crucially on the value of the spin, revealing the subtle workings of the spin Berry phases (see, e.g., Ref. 32 and references therein). For $S=\frac{1}{2}$ these act to give a special stability to "valence-bond" pair singlets involving nearest-neighbor spins, and the quantum-disordered phases are actually valence-bond crystals breaking the translational symmetry of the square lattice further to fourfold degenerate spin-Peierls states. But for $S=1$ the Berry phases act in favor of the formation of "chain singlets"[30,31] that can stack either along the x or y direction of the square lattice yielding a twofold degenerate ground state.

In this paper we investigate the $S=1$ version of the spatially anisotropic J_1-J_2 model given by the Hamiltonian

$$H = J_{1x} \sum_{\langle i,j\rangle_x} \mathbf{S}_i \mathbf{S}_j + J_{1y} \sum_{\langle i,j\rangle_y} \mathbf{S}_i \mathbf{S}_j + J_2 \sum_{\langle\langle i,j\rangle\rangle} \mathbf{S}_i \mathbf{S}_j, \qquad (1)$$

where the first two sums run over NN spins with exchange couplings $J_{1x} \leq J_{1y}$ in x and y directions, respectively, and the third sum runs over all NNN pairs with exchange couplings J_2 as illustrated in Fig. 1. We note that both the spatially isotropic J_1-J_2 model as well as the decoupled Haldane spin-chain limit appear as special cases of Hamiltonian (1).

Unlike for $S=\frac{1}{2}$ this model has been hardly explored for $S=1$ despite the potential relevance for the iron pnictides, and to best of our knowledge exact diagonalization studies are not available. In a very recent coupled cluster treatment[33] it has been found that at the isotropic point $J_{1x}=J_{1y}=J_1$ the Néel and stripe ordered phases are separated by a first-order transition at $J_2/J_1 \approx 0.55$ slightly smaller than the MSWT (Refs. 14 and 15) and SBMFT (Ref. 16) results and that the transition remains first order up to an anisotropy $J_{1x}/J_{1y} \approx 0.66$. For stronger anisotropies the authors find continuous transitions very close to the classical transition line $J_2=J_{1x}/2$ although they were not able to resolve an intermediate paramagnetic region within the numerical resolution. On contrary, a two-step density-matrix renormalization-group (DMRG) study[34] at the particular point $J_{1x}/J_{1y}=0.2$ indicated a much wider nonmagnetic region with a spin-gap reaching its maximum $\Delta \approx 0.39 J_{1y}$ close to the maximally frustrated point $J_2/J_{1y}=0.1$, which is only slightly below the gap $\Delta_H \approx 0.41J$ (Ref. 35) of an isolated Haldane chain.[36,37]

Starting from the Haldane chain limit ($J_{1x}=J_2=0$) it has been predicted by the Monte Carlo simulations[38] as well as analytically[39] that an infinitesimal coupling J_{1x} leads to the destruction of the topological string order[40] of the Haldane chain. However, due to the protection by the finite energy gap of the spin-1 Haldane chain all other ground-state properties as well as the thermodynamics are only minimally affected by a small interchain coupling J_{1x} and a finite, albeit small[41–44] coupling is necessary to establish magnetic long-range order. Whereas a similar reasoning should hold for a vanishing NN coupling perpendicular to the chains ($J_{1x}=0$) and small diagonal coupling J_2, the Haldane chain phase seems to be considerably more stable against the simultaneous increase of the two mutually frustrating couplings J_{1x} and J_2 as indicated by two-step DMRG results showing an almost negligible reduction in the spin gap for moderate interchain couplings.[34] This suggests that the paramagnetic phase of the frustrated two dimensional spin model can be viewed as a continuation of the Haldane spin chain. Recently, based on a theoretical method with a continuous deformation of the J_1-J_2 model, the ground state at the special isotropic case $J_2=J_1/2$ has been conjectured[45] to be a twofold degenerate valence-bond solid state along either the horizontal or vertical direction of the square lattice. The main result of this paper is that by employing DMRG and by studying systematically how matters evolve as function of increasing anisotropy we arrive at solid evidence for the smooth continuation between the Haldane chain phase and an isotropic disordered phase near $J_2=J_1/2$.

Since for $S=1$ exact diagonalization is restricted to very small system sizes and since the quantum Monte Carlo (QMC) method suffers from the infamous sign problem in the presence of frustration we employ the DMRG method[46] to map out the phase diagram of the spatially anisotropic J_{1x}–J_{1y}–J_2 model [Eq. (1)] over the whole parameter range including the decoupled Haldane spin chains and the isotropic J_1-J_2 model as limiting cases. The DMRG has the merits of not being biased as analytical treatments based on $1/S$ or $1/N$ expansions, being capable of dealing with frustrated systems and allowing to investigate much bigger system than possible with exact diagonalization. Moreover, it is capable of reproducing the spin gap of the decoupled Haldane chain limit with high accuracy.[34] The resulting phase diagram is contrasted by analytical results we obtain within a generalization of the SBMFT to the anisotropic system.

The remainder of the paper is organized as follows. In Sec. II we outline the SBMFT and calculate the resulting phase diagram which is used for comparison with the numerical results. In Sec. III we use the DMRG to construct the phase diagram by a careful finite-size analysis of the magnetic structure factor at the ordering wave vectors of the two magnetically ordered phases as well as of the spin gap in the

nonmagnetic region as a function of the NNN coupling J_2 for various ratios of the NN couplings J_{1x} and J_{1y}. Finally, in Sec. IV the results obtained within the two methods are compared and the shortcomings of the semiclassical approach are highlighted. Further, the potential relevance of our findings for the iron pnictides is discussed.

II. SBMFT

In this section we generalize the SBMF calculation for the isotropic J_1-J_2-model[16] to the case of anisotropic nearest-neighbor exchange couplings. For abbreviation we define $J_x := J_{1x}$, $J_y := J_{1y}$, and $J_d := J_2$. Assuming $J_x \leq J_y$, the classical ground states are given by a Néel-ordered state with an ordering wave vector $\boldsymbol{Q}=(\pi,\pi)$ for $J_d/J_x \leq 1/2$ and by a columnar antiferromagnetic state with $\boldsymbol{Q}=(0,\pi)$ for $J_d/J_x > 1/2$. Following the previous calculations, we perform a spin rotation $\tilde{S}_i^x = \sigma_i S_i^x$, $\tilde{S}_i^y = \sigma_i S_i^y$, and $\tilde{S}_i^z = S_i^z$, where $\sigma_i = \exp(i\boldsymbol{Q}\boldsymbol{r}_i) = \pm 1$, with $\boldsymbol{Q}$ as the ordering wave vectors of the two classical orders, and represent the rotated spin operators in terms of Schwinger bosons $b_{i,\uparrow}$ and $b_{i,\downarrow}$ as

$$\tilde{\boldsymbol{S}}_i = \frac{1}{2} b_{i,\nu}^\dagger \boldsymbol{\sigma}_{\nu,\nu'} b_{i,\nu'}. \tag{2}$$

Here $\boldsymbol{\sigma}=(\sigma^x,\sigma^y,\sigma^z)$, with σ^α the standard Pauli matrices. The constraint $b_{i,\nu}^\dagger b_{i,\nu}=2S$ ensures that $\langle \boldsymbol{S}^2 \rangle = S(S+1)$. Hamiltonian (1) can then be rewritten in the compact form

$$\mathcal{H} = \frac{1}{2}\sum_{(i,j)} J_{ij}\left[\frac{\sigma_i\sigma_j+1}{2}(F_{ij}^\dagger F_{ij} - 2S^2) + \frac{\sigma_i\sigma_j-1}{2}(G_{ij}^\dagger G_{ij} - 2S^2)\right], \tag{3}$$

where the sum runs over all bonds, and we have introduced the bond operators $F_{ij}^\dagger = b_{i,\nu}^\dagger b_{j,\nu}$ and $G_{ij}^\dagger = b_{i,\nu}^\dagger b_{j,-\nu}^\dagger$. A mean-field decoupling is then performed with respect to the order parameters $f_{ij}=\langle F_{ij}^\dagger \rangle/2$ and $g_{ij}=\langle G_{ij}^\dagger \rangle/2$. For the Néel-ordered phase we have to introduce fields g_x and g_y for the nonfrustrated nearest-neighbor bonds and f_d for frustrated NNN bonds, whereas the $(0,\pi)$ phase is characterized by order-parameter fields g_y and g_d for the nonfrustrated bonds along the y and diagonal directions and f_x for the frustrated x bonds. The local constraints are replaced by a global one and treated with a Lagrange multiplier λ. The resulting mean-field Hamiltonian, which in momentum space is given by

$$\mathcal{H}_{\mathrm{mf}} = \int_{\boldsymbol{q}} [(h_{\boldsymbol{q}}+\lambda)(b_{\boldsymbol{q}\uparrow}^\dagger b_{\boldsymbol{q}\uparrow} + b_{-\boldsymbol{q}\downarrow}^\dagger b_{-\boldsymbol{q}\downarrow}) - \Delta_{\boldsymbol{q}}(b_{\boldsymbol{q}\uparrow}^\dagger b_{-\boldsymbol{q}\downarrow}^\dagger + b_{\boldsymbol{q}\uparrow} b_{-\boldsymbol{q}\downarrow})], \tag{4}$$

is easily diagonalized by a Bogolioubov transformation yielding the dispersion

$$\omega_{\boldsymbol{q}} = [(h_{\boldsymbol{q}}+\lambda)^2 - \Delta_{\boldsymbol{q}}^2]^{1/2}, \tag{5}$$

with

$$h_{\boldsymbol{q}} = 4 f_d J_d \cos q_x \cos q_y, \tag{6a}$$

$$\Delta_{\boldsymbol{q}} = 2(g_x J_x \cos q_x + g_y J_y \cos q_y) \tag{6b}$$

in the Néel phase and likewise in the $(0,\pi)$ phase

$$h_{\boldsymbol{q}} = 2 f_x J_x \cos q_x, \tag{7a}$$

$$\Delta_{\boldsymbol{q}} = 2 g_y J_y \cos q_y + 4 g_d J_d \cos q_x \cos q_y. \tag{7b}$$

The Lagrange multiplier in the ordered phases is determined by the requirement that $\omega_{\boldsymbol{Q}}=0$ for the corresponding ordering wave vectors yielding $\lambda = 2(g_x J_x + g_y J_y) - 4 f_d J_d$ in the Néel and $\lambda = 2(g_y J_y - f_x J_x) + 4 g_d J_d$ in the $(0,\pi)$ phase. The reduced moment S^* in the ordered phases is determined by

$$S^* = S - \frac{1}{2}\left(\int_{\boldsymbol{q}} \frac{h_q+\lambda}{\omega_q} - 1\right). \tag{8}$$

Naturally, one might expect that quantum fluctuations tend to destabilize the classical orders introducing an intermediate paramagnetic phase. In this case the second-order transitions between the two different magnetic orders are determined by the lines where the corresponding magnetizations go to zero, $S^* \to 0$. However, the analysis of the isotropic model[16] ($J_x = J_y$) shows that the quantum fluctuations can lead to a significant stabilization of the Néel order leading to a region where $S^*_{(\pi,\pi)} > 0$ and $S^*_{(0,\pi)} > 0$. In this region which is expected to persist for not too strong anisotropy, a discontinuous first-order transition between the two different magnetic orders is likely and can be estimated from a comparison of the ground-state energies which immediately follow from Eq. (3) as

$$E_{(\pi,\pi)} = -J_x(2g_x^2 - S^2) - J_y(2g_y^2 - S^2) + 2J_d(2f_d^2 - S^2), \tag{9a}$$

$$E_{(0,\pi)} = J_x(2f_x^2 - S^2) - J_y(2g_y^2 - S^2) - 2J_d(2g_d^2 - S^2). \tag{9b}$$

The order-parameter fields entering the mean-field Hamiltonian [Eq. (4)] have to be determined self-consistently. Using the above Bogoliubov transformation we obtain for the Néel-ordered phase

$$g_x = S^* + \int_{\boldsymbol{q}} \frac{\Delta_q}{2\omega_q}\cos q_x, \tag{10a}$$

$$g_y = S^* + \int_{\boldsymbol{q}} \frac{\Delta_q}{2\omega_q}\cos q_y, \tag{10b}$$

$$f_d = S^* + \int_{\boldsymbol{q}} \frac{h_q+\lambda}{2\omega_q}\cos q_x \cos q_y, \tag{10c}$$

whereas in the $(0,\pi)$ phase the self-consistency equations for the order-parameter fields are given by

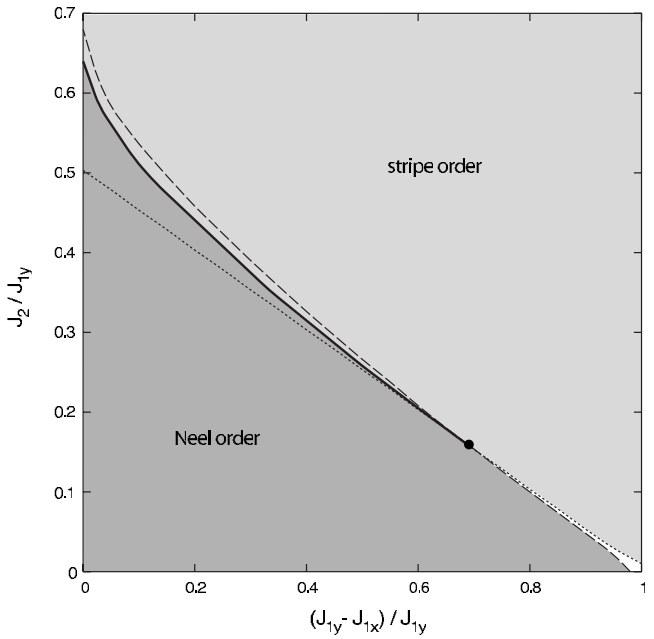

FIG. 2. Phase diagram for $S=1$ as a function of and anisotropy $\alpha=(J_{1y}-J_{1x})/J_{1y}>0$ between the nearest-neighbor exchange couplings and relative strength of the next-nearest-neighbor coupling J_2/J_{1y} obtained within SBMFT. Up to an anisotropy $\alpha\approx 0.66$ the (π,π) and $(0,\pi)$ antiferromagnetic orders are separated by a first-order transition (solid line). At the tricritical point the first-order line splits into two second-order lines (dashed and dotted) separating the two magnetic phases from a gapped nonmagnetic phase.

$$f_x = S^* + \int_{\boldsymbol{q}} \frac{h_{\boldsymbol{q}} + \lambda}{2\omega_{\boldsymbol{q}}} \cos\, q_x, \tag{11a}$$

$$g_y = S^* + \int_{\boldsymbol{q}} \frac{\Delta_{\boldsymbol{q}}}{2\omega_{\boldsymbol{q}}} \cos\, q_y, \tag{11b}$$

$$g_d = S^* + \int_{\boldsymbol{q}} \frac{\Delta_{\boldsymbol{q}}}{2\omega_{\boldsymbol{q}}} \cos\, q_x \cos\, q_y. \tag{11c}$$

The resulting phase diagram for $J_{1x}\leq J_{1y}$ is shown in Fig. 2 as a function of the anisotropy $\alpha=(J_{1y}-J_{1x})/J_{1y}$ between the NN exchange couplings and of the relative strength $\beta=J_2/J_{1y}$ of the NNN coupling. In agreement with earlier studies of the isotropic limit $J_{1x}=J_{1y}=J_1$ within SBMFT and MSWT, we find a dramatic stabilization of the Néel order above the classical value and a large region $0.51\lesssim\beta\lesssim 0.68$ where the two competing orders are potentially stable, indicated by $S^*_{(\pi,\pi)}>0$ and $S^*_{(0,\pi)}>0$. The crossing of the self-consistently determined energies of the two states suggests a first-order transition at $\beta\approx 0.64$ considerably larger than the classical value 1/2 and about 10% bigger than the coupled cluster result.[33] Although the region of coexistence is considerably narrowed by a small anisotropy, we find it to persist up to $\alpha\approx 0.66$ where the first-order line terminates. The existence of such a tricritical point was also suggested by the coupled cluster analysis although located at a much smaller anisotropy $\alpha\approx 0.34$. For anisotropies $\alpha>0.66$ we find an intermediate nonmagnetic region $(S^*_{(\pi,\pi)}=S^*_{(0,\pi)}=0)$ separating the two ordered phases. This region is found to be very narrow and close to the classical phase boundary $\beta=(1-\alpha)/2$.

Although the existence of a tricritical point and of a very narrow paramagnetic strip terminating at the Haldane chain limit $J_{1x}=J_2=0$ is in qualitative agreement with the coupled cluster results[33] the small width of the paramagnetic region is in disagreement with other available numerical results. For $J_{1x}/J_{1y}=0.2$ $(\alpha=0.8)$ a two-step DMRG calculation[34] shows a much wider nonmagnetic region centered around the classical transition point $J_2/J_{1y}=0.1$. Interestingly, the spin gap at this maximally frustrated point is almost identical to that of an isolated Haldane chain suggesting that even for relatively strong interchain couplings one-dimensional Haldane chain physics is still important. This is certainly missed by the SBMF calculation which treats the spin as a continuous variable and does not distinguish between integer and half-integer spins crucial for the existence of the Haldane spin gap. Moreover, it has been established within quantum Monte Carlo calculations[41–43] that for $J_2=0$ the transition between the Néel ordered phase and the gapped nonmagnetic phase is located at $J_{1x}/J_{1y}=0.044$, again indicating that the paramagnetic region close to the Haldane chain limit is considerably wider than suggested by both the SBMFT and the coupled cluster results.[33] Since for $J_2=0$ the system is not frustrated quantum Monte Carlo can be considered exact in this regime.

We have also calculated the transition out of the $(0,\pi)$ state in linear spin-wave theory for comparison to the SBMFT calculation and to preliminary neutron-scattering results on the pnictides that found $(0,\pi)$ order but with a small moment. This method computes the reduction of the classical antiferromagnetic moment due to zero-point excitations of spin waves (which captures the $1/S$ correction to the classical moment in a large-S expansion). The transition line out of the ordered phase is estimated as the point where the correction is as large as the original moment.

We assume three antiferromagnetic couplings: J_{1x}, J_{1y}, and J_2, with $J_{1y}>J_{1x}$, and that we are in a $(0,\pi)$ ordered phase, which requires (as is evident from the formula below) that $J_{1x}<2J_2$. The dispersion relation for spin-wave excitations was previously obtained for this anisotropic J_1-J_2 model in Ref. 10. The integral for the correction to the classical moment around the $(0,\pi)$ case is, in units of the Bohr magneton and with lattice spacing $a=1$,

$$\Delta m = \int_{[0,2\pi]^2} \frac{d^2\mathbf{k}}{(2\pi)^2}\left(\frac{1}{\sqrt{1-\cos^2(k_y)/f(k_x)^2}}-1\right), \tag{12}$$

with

$$f(k_x) = \frac{2J_2 + J_{1y} - J_{1x}[1-\cos(k_x)]}{2J_2\cos(k_x) + J_{1y}}. \tag{13}$$

The transition is found numerically to lie very close to the classical transition line $J_{1x}=2J_2$: the normalized difference $(J_2^c - J_{1x}/2)/J_{1y}$, where J_2^c is the critical coupling where the correction is equal to the original moment, is always less than 2% for $0<J_{1x}<0.99J_{1y}$. Significant reduction in the

ordered moment also occurs only near the classical transition line. The primary difference from the SBMFT calculation is that the spin-wave calculation always predicts a paramagnetic phase between stripe and Neél order. The width of this paramagnetic phase is much smaller in either approach than in the DMRG calculation of the following section because these analytical approaches do not capture the strong quantum fluctuations that favor the Haldane phase.

III. DMRG

The above SBMFT has clearly shown an interesting narrow boundary region between the Néel and stripe ordered phases in the phase diagram of Fig. 2, where the quantum fluctuations are expected to become very important. Most interestingly, it suggests an increasing tendency towards a fluctuation induced first-order transition on approaching the isotropic point $J_{1x}=J_{1y}$. However, the comparison with previous numerical results[34,41–43] indicates that the SBMFT tends to overestimate the stability of the magnetically ordered phases, surely close to the Haldane chain limit but presumably also for larger values of J_{1x} and J_2. In the following we shall refine the boundary region by using DMRG method.

In the following DMRG calculation, we will set $J_{1y}=J_1$ as an energy unit, and a periodic boundary condition (PBC) is used and in each DMRG block up to $m=3200$ states are to be kept with the truncation error in the order of or less than 10^{-5}.

A. Isotropic case with $J_{1x}=J_{1y}=J_1$

Let us first consider the isotropic case $J_{1x}=J_{1y}=J_1$ where the SBMFT suggests the strongest tendency towards a first-order transition although the transition point $J_2/J_1\approx 0.64$ obtained from a comparison of the energy minima seems to be suspiciously high compared to the classical transition point $J_2/J_1=0.5$. Figure 3(a) shows the ground-state energy per site calculated by DMRG with the sample size varying from $N=4\times 4$ (16 sites) up to $N=8\times 8$ (64 sites). The ground-state energy reaches the maximum with J_2 between $0.54J_1$ and $0.58J_1$, which becomes sharper with the increase in sample size, indicating a region with possible phase transitions below the first-order transition point obtained in SBMFT but still notable above the classical transition. As shown in Fig. 3(b), we also calculate the ground-state energy per site and the spin-1 gap as a function of the truncation error in the isotropic case with $J_2/J_1=0.54$, which has the largest spin-1 gap. From the figure we can see that E_0/N shows a linear relation with the truncation error. Most importantly, the spin-1 gap converges to a constant with decreasing the truncation error, which gives us the reliable results in the large m limit.

We examine such a region by calculating the magnetic structure factor $S_z(\mathbf{q})$ defined by

$$S_z(\mathbf{q})=\frac{1}{N}\sum_{i,j} e^{-i\mathbf{q}(\mathbf{r}_i-\mathbf{r}_j)}\langle S_i^z S_j^z\rangle.$$

As expected, we find that $S_z(\mathbf{q})$ shows a dramatic change from peaking at $\boldsymbol{Q}=(\pi,\pi)$ (the Néel order) to $\boldsymbol{Q}=(0,\pi)$ (the stripe order) with increasing J_2/J_1. Figs. 4(a) and 4(b) illustrate $S_z(\mathbf{q})/N$ vs J_2/J_1 for system sizes $N=4\times 4$, 6×6, and 8×8, as well as the thermodynamic limit values obtained by a finite-size scaling. Here we have used the quadratic function $f(x)=A+Bx+Cx^2$, with $x=\frac{1}{N}$ to perform the finite-size scaling.

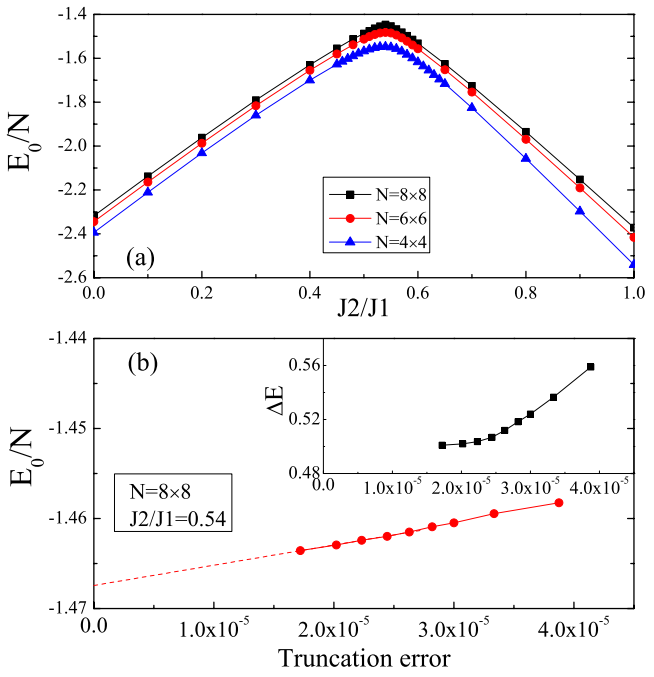

FIG. 3. (Color online) (a) The ground-state energy per site E_0/N at different system size $N=4\times 4$ (blue triangle), 6×6 (red circle), and 8×8 (black square) for the isotropic case with $J_{1x}=J_{1y}=J_1$. (b) Ground-state energy per site E_0/N at $N=8\times 8$ as a function of the truncation error. The dashed line is the extrapolation to zero error limit. Inset: the spin-1 gap ΔE as a function of the truncation error.

The Néel order transition point is found at $J_2/J_1\approx 0.525$ in Fig. 4(a), which is clearly distinct from the stripe order

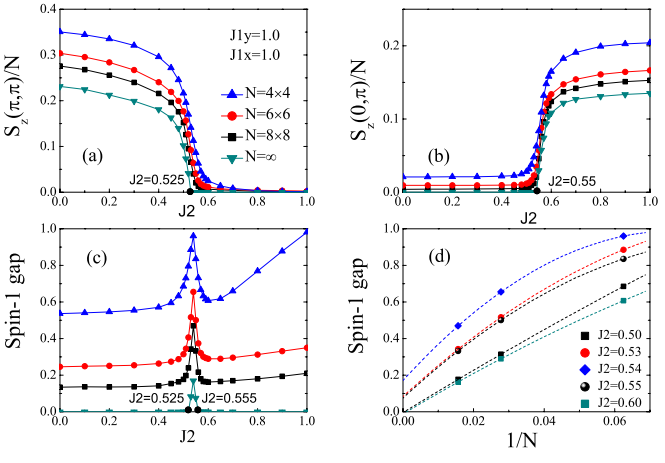

FIG. 4. (Color online) The evolution of the peak values of the structure factors, (a) $S_z(\pi,\pi)/N$, (b) $S_z(0,\pi)/N$, and (c) of the spin-1 gap, at three different size $N=4\times 4$, 6×6, and 8×8, as well as their thermodynamic limit extrapolations in the isotropic case $J_{1x}=J_{1y}=J_1=1$. The finite-size scaling for the spin-1 gap is shown in (d).

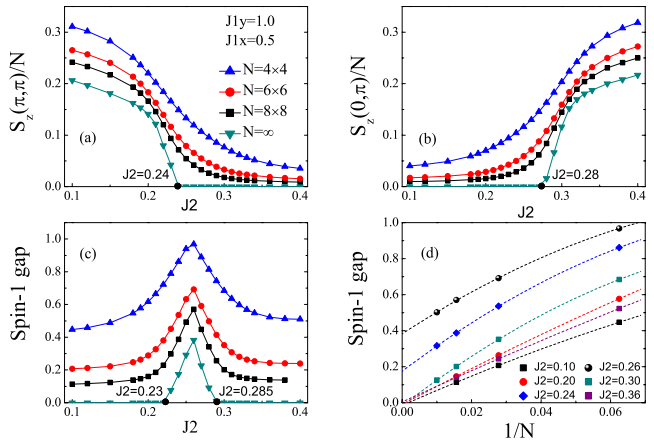

FIG. 5. (Color online) The peak values, (a) $S_z(\pi,\pi)/N$, (b) $S_z(0,\pi)/N$, and (c) the spin-1 gap, versus J_2/J_{1y} at $J_{1x}/J_{1y}=0.5$ for different sizes. The finite-size scaling for the spin-1 gap is shown in (d).

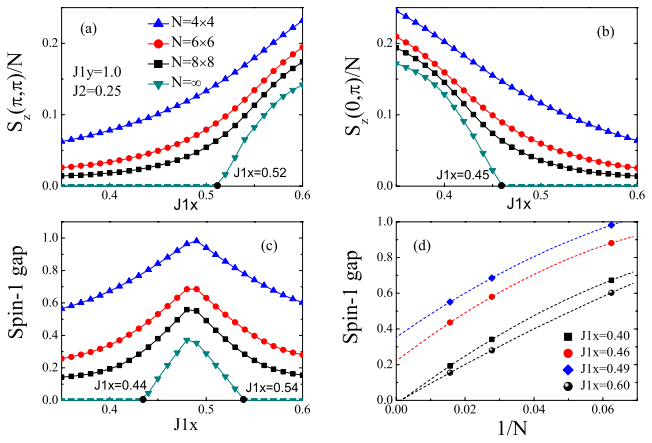

FIG. 6. (Color online) (a) $S_z(\pi,\pi)/N$, (b) $S_z(0,\pi)/N$, and (c) the spin-1 gap, versus J_{1x}/J_{1y} at $J_2/J_{1y}=0.25$ for different sample sizes. In (d), the finite-size scaling for the spin-1 gap is given.

transition point at $J_2/J_1\approx 0.55$ in Fig. 4(b) indicating that the two magnetically ordered phases are separated by an intermediate nonmagnetic region.

To independently verify the above results, we also calculate the spin-1 gap $\Delta E(S=1)\equiv E_1(S=1)-E_0$ presented in Figs. 4(c) and 4(d). Figure 4(d) illustrates the finite-size scaling for the spin gap $\Delta E(S=1)$ at different values of J_2 using a scaling function $f(x)$. In Fig. 4(c), the evolution of the spin-1 gap as a function of J_2 is given. In the thermodynamic limit, the transition points determined by the spin-1 gap are at $J_2\approx 0.525$ and $J_2\approx 0.555$, respectively, which are very close to the previous results determined by the structure factor. Therefore, for the present $S=1$ J_1-J_2 model in the isotropic limit, our numerical approach has established an intermediate spin-disordered region with a finite spin gap which separates the two ordered magnetic phases.

B. Anisotropic case with $J_{1x}<J_{1y}=J_1$

Now we consider how the spin-disordered phase evolves with the increase in anisotropy at $J_{1x}<J_{1y}=J_1$. First we consider the case at $J_{1x}=0.5J_1$, and the results are presented in Fig. 5. By using the same finite-size scaling procedure, we find that the spin-disordered phase is bound by a lower transition point $J_2/J_1\approx 0.24$ and an upper transition point $J_2/J_1\approx 0.28$ based on the structure factor calculation. Again the spin gap calculation gives rise to a consistent spin-disordered regime between $J_2/J_1\approx 0.23$ and $J_2/J_1\approx 0.285$ as shown in Fig. 5(c).

In the same regime, with a fixed $J_2/J_1=0.25$, we have further studied the phase boundaries by varying J_{1x}/J_1. As shown in Fig. 6, the lower transition point is obtained at $J_{1x}/J_1=0.45$ and the upper transition point at $J_{1x}/J_1\approx 0.52$, while the finite-size scaling for the spin-1 gap results in a similar region between $J_{1x}/J_1=0.44-0.54$.

In the extreme case at $J_{1x}=0$ and $J_2=0$ with $J_{1y}=J_1$, the system simply reduces to an array of decoupled $S=1$ spin chains with a finite Haldane gap. Figure 7 shows how the ground state continuously evolves from that of the well-known decoupled spin chains to the anisotropic two-dimensional (2D) case by turning on J_{1x}/J_1, which remains disordered until the Néel order sets in at $J_{1x}/J_1\approx 0.05$ with $S_z(\pi,\pi)/N$ becoming finite in the thermodynamic limit. Indeed the corresponding spin-1 gap continuously decreases with the turning on of a finite J_{1x} but only vanishes around $J_{1x}/J_1\approx 0.06$ as shown in Figs. 7(c) and 7(d).

Now we turn on J_2. At $J_{1x}=0$, we find that while the calculated structure factor at (π,π) continuously reduces as the sample size increases from $N=4\times 4$, 6×6, to 8×8, and is extrapolated to zero by finite-size scaling, a finite stripe order $S_z(0,\pi)/N$ will emerge at $J_2/J_{1y}=0.025$ in the thermodynamic limit, which is further supported by vanishing spin-1 excitation gap at the same point as shown in Fig. 8. It is noted that the best finite scaling for the structure factor here is obtained with using a $f(x)$, with $x=1/\sqrt{N}=1/N_y$, for a square lattice $N_x=N_y$, instead of $x=1/N$ used previously. The justification of such a finite-size scaling for the spin structure factors at $J_{1x}=0$ and small J_2/J_{1y} is given in Fig. 9 and its caption.

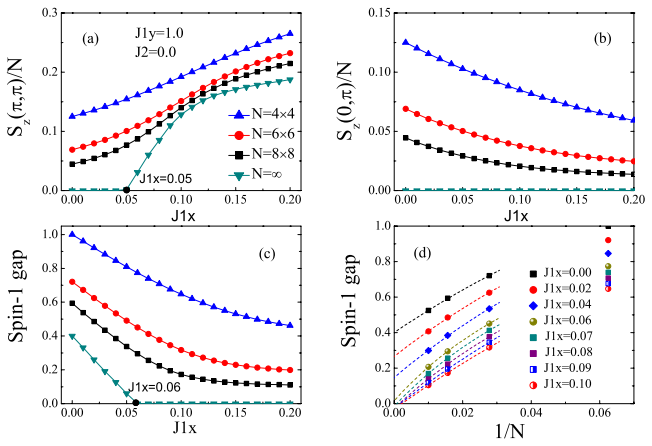

FIG. 7. (Color online) (a) $S_z(\pi,\pi)/N$, (b) $S_z(0,\pi)/N$, and (c) the spin-1 gap, versus J_{1x}/J_{1y} at $J_2=0$ at different sizes. In (d), the finite-size scaling for the spin-1 gap is given.

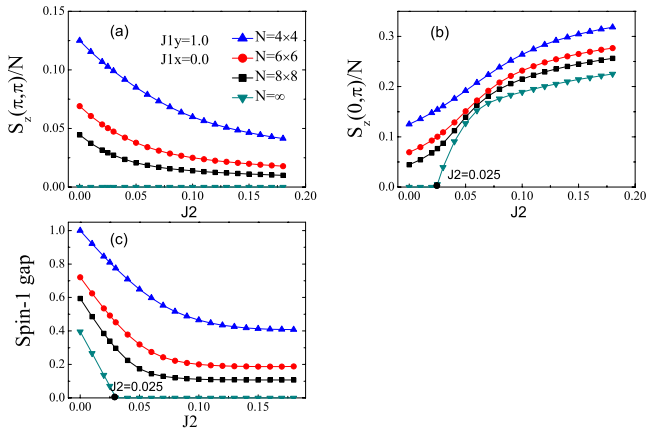

FIG. 8. (Color online) At $J_{1x}=0$, the structure factors (a) $S_z(\pi,\pi)/N$ and (b) $S_z(0,\pi)/N$ as well as the (c) spin-1 gap versus J_2/J_{1y} are shown at different sizes, including their thermodynamic extrapolations.

C. Phase diagram

The resulting phase diagram obtained by the DMRG calculations with careful finite-size scalings of the magnetic structure factor as well as the spin gap is shown in Fig. 10 as a function of the anisotropy $\alpha=(J_{1y}-J_{1x})/J_{1y}$ between the NN couplings and the relative strength $\beta=J_2/J_{1y}$ of the NNN superexchange.

In contrast to the SBMFT which in the regime of small anisotropy α suggests a first-order transition between the Néel- and stripe-ordered phases (see Fig. 2), the DMRG results clearly indicate a paramagnetic strip separating the two magnetically ordered phases for all values of the anisotropy α including the isotropic point $J_{1x}=J_{1y}$ ($\alpha=0$). With increasing α the width of this region is found to slightly increase. Close to the Haldane chain limit the SBMFT predicts an intermediate nonmagnetic phase although the width of this region is found to be much larger in the DMRG calculation in quantitative agreement with a previous two-step DMRG analysis at fixed $\alpha=0.8$ (Ref. 34).

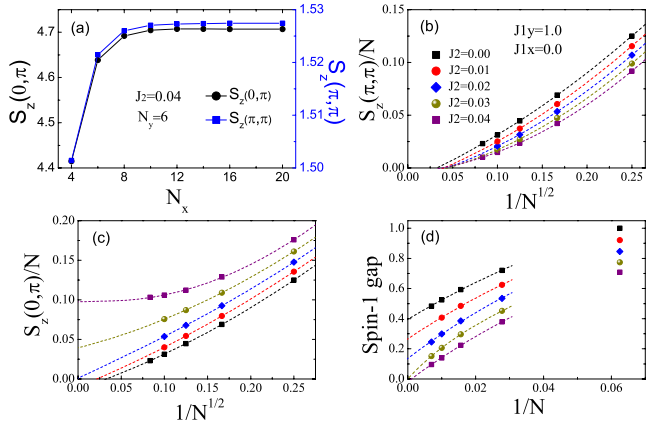

FIG. 9. (Color online) (a) The size dependence of the structure factor [for a given $N_y=6$ (six-leg systems)] at $J_{1x}=0$ and small J_2/J_{1y} which quickly saturates at $N_x>N_y$, indicating that $x=1/N_y$ in the scaling function $f(x)$ for the structure factor is more appropriate in this extreme limit. The corresponding finite-size scaling of the structure factors for square samples are illustrated in (b) and (c), respectively. For comparison, the spin-1 gap at different J_2 is still well scaled by $x=1/N$ in the scaling function as shown in (d).

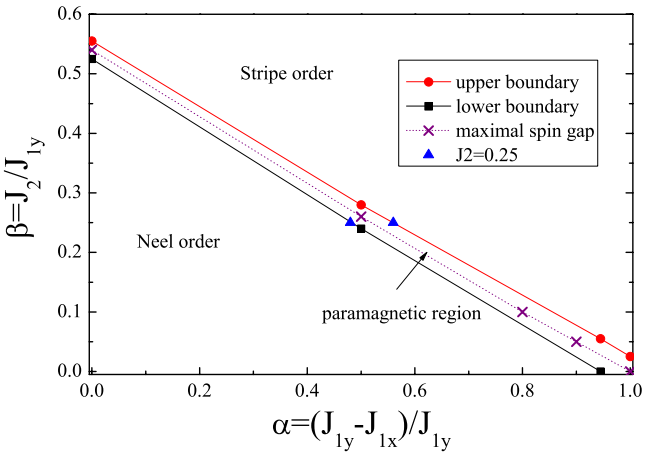

FIG. 10. (Color online) Phase diagram for the anisotropic J_1-J_2 model determined by DMRG. The Néel order and stripe order phases are separated by a paramagnetic regime with the boundaries denoted by the red line with full circles for the upper and the blank line with full squares for the lower transition points, respectively. In the middle of the paramagnetic region lies in a dotted line with crosses which marks the maximal spin-1 gap $\Delta E_{\max}$. Note that the symbols of circle, square, and triangular denote the phase-transition points determined by DMRG in the previous figures.

For $J_2=0$ we can compare our results to recent QMC simulations,[41–43] which in this regime can be considered exact since the system is not frustrated and QMC is therefore free of any sign problem. Within DMRG we find the transition between the gapped Haldane phase and the Néel-ordered phase to occur at $J_{1x}/J_{1y}\approx 0.05$ (see Fig. 10) in good agreement with QMC transition point $J_{1x}/J_{1y}=0.044$. Moreover, in the Haldane chain limit $J_{1x}=J_2=0$ we obtain a spin gap $\Delta\approx 0.4$ [see Fig. 7(d)] very close to the exact value $\Delta_H=0.41$ for the Haldane spin chain,[35] again demonstrating that the finite-size scaling is well converged.

Very interestingly, starting from the Haldane chain limit we find the maximum spin gap in the paramagnetic phase to decrease only very slowly with increasing couplings J_{1x} and J_2. Up to $J_{1x}/J_{1y}=0.5$, the gap is almost identical to the Haldane spin gap [see Fig. 5(d)] indicating that the Haldane spin chain is very robust against the simultaneous increase in the mutually frustrating couplings J_{1x} and J_2. Remarkably, even the paramagnetic phase of the isotropic J_1-J_2 model with a maximum spin gap still being about half of the Haldane gap is continuously connected to the Haldane spin-chain limit.

At the isotropic point $J_{1x}=J_{1y}$ ($\alpha=0$) we find an intermediate paramagnetic phase for $0.525\lesssim J_2/J_1\lesssim 0.555$. This region is considerably smaller than in the $S=\frac{1}{2}$ case, where a paramagnetic regime $0.4\lesssim J_2/J_1\lesssim 0.6$ presumably with columnar valence-bond order has been established by various numerical methods.[18–28] Interestingly, the stabilization of the Néel phase above the classical transition point is in agreement with the SBMFT. Furthermore, we also calculate the lowest spin singlet excitation gap for the system $N=4\times 4$ by

means of ED, which becomes very small in the intermediate region. Very interestingly, a small perturbation term added to the Hamiltonian that breaks the rotational symmetry of the lattice can lead to a two-fold near degenerate ground state. Most importantly, in the zero perturbation limit, our calculations show an increasing tendency that a twofold degenerate ground state spontaneously breaks the lattice rotation may exist. However, due to the limitation of DMRG method in calculating the excited state of the 2D systems, we are not able to fully investigate this issue at larger system sizes.

Despite the apparent failure of the semiclassical SBMFT in dealing with the strong quantum fluctuations in the boundary region between the two magnetically ordered phases it is interesting to note that the paramagnetic region covers the phase boundaries obtained by SBMFT for the most of $J_{1x} < J_{1y}=J_1$ region except for the part close to the isotropic limit and that the points where the spin gap is maximum (indicated by crosses and dotted in Fig. 10) are almost on top of both the first-order transition line as well as of the two narrow second-order lines obtained within SBMFT.

IV. DISCUSSION

In summary, we have studied the frustrated spin-1 Heisenberg $J_{1x}-J_{1y}-J_2$ model on a square lattice numerically using the DMRG method and analytically employing the Schwinger-Boson mean-field theory (SBMFT). Interestingly, this model contains both the isotropic J_1-J_2 model as well as decoupled Haldane spin chains as limiting cases. Moreover, it has attracted a lot of attention recently since it has been motivated as an effective model to describe the $(0,\pi)$ magnetism and the low-energy spin-wave excitations of the celebrated iron pnictide superconductors. Furthermore it has been suggested that the drastic reduction in magnetic moments to a value of $0.4\mu_B$ is caused by strong quantum fluctuations in the vicinity of a continuous phase transition. However, to the present day the phase diagram has not been determined yet.

Within both the SBMFT and the DMRG we find that the Néel phase is stabilized considerably by quantum fluctuations above the classically stable region up to a relatively strong anisotropy between the NN couplings. However, in all other regards the phase diagrams obtained by the two methods clearly disagree, indicating the importance of the strong quantum fluctuations.

The SBMFT suggest a fluctuation-induced first-order transition between the Néel and the stripe antiferromagnets terminating at a tricritical point and splitting into two second-order lines separated by an intermediate paramagnetic region only for large anisotropies. Although the existence of a tricritical point and a hardly sizable paramagnetic strip terminating at the decoupled Haldane spin chain point $(J_{1x}=J_2=0)$ are consistent with a recent coupled cluster calculation,[33] the SBMFT definitely falls short on approaching the Haldane chain limit. This becomes clear by a comparison with quantum Monte Carlo simulations[41–43] showing a much larger region of stability of the Haldane chain phase against interchain couplings J_{1x}. Also the previous two-step DMRG calculation[34] at $J_{1x}/J_{1y}=0.2$ indicates a paramagnetic region being an order of magnitude wider than found within the SBMFT.

On the contrary, the phase diagram obtained within DMRG by a careful finite-size scaling of the magnetic structure factor and the spin gap is consistent with both the QMC and the previous DMRG results. Furthermore the spin gap in the decoupled chain limit agrees well with the exact value for the isolated Haldane chain. It also agrees excellently with the work of Sato and Oshikawa,[47] who studied the weakly coupled Haldane chains. The width of the paramagnetic region slightly decreases on approaching the isotropic point but remains finite over the entire parameter range. This has the remarkable implication that the paramagnetic phase of the frustrated two-dimensional spin model, including the isotropic J_1-J_2 limit, is continuously connected to the Haldane spin-chain phase. In other words, the paramagnetic phase can be viewed as a continuation of the Haldane spin chain phase, with the caveat that the topological string order has to disappear at any finite interchain coupling.[38,39]

The reason for the failure of the semiclassical SBMFT in dealing correctly with the strong quantum fluctuations in the boundary region between the two classical orders is easy to understand. The SBMFT deals with the spin as continuous variable while it is *blind for the Berry phase effects* that distinguish between half-integer and integer spin values crucial for the existence of the Haldane gap as well the valence-bond crystals. This physics is definitely missed by the semiclassical treatment. Our DMRG results demonstrates that the Haldane chain phase is very robust against the simultaneous increase of the couplings J_{1x} and J_2 along the strongly frustrated boundary region, indicated by the minute reduction in the spin gap compared to the isolated Haldane chain limit. Similar results are found in a similar model but with $S=1/2$ spins,[48] where the two classical phases, Neel and stripe, are separated by the quantum-disordered phase centered on line $J_{1x}=2J_2$.

What does the study of this spin system teach us regarding the superconductivity in the iron pnictides? One could speculate that the basic physics is similar as in the cuprates. Although the spins are larger in the pnictides, the geometrical frustration renders the spin system to be on the verge of undergoing a quantum phase transition in a quantum-disordered state. This quantum spin physics then sets the conditions for the emergence of superconductivity in the doped systems. But in this regard the size of the microscopic spin does matter more than one intuitively anticipates. For $S=1/2$ the well established fact that the Berry phases conspire to turn the quantum-disordered states of the spin-only systems into valence-bond solids gives a rationale to take Anderson's resonating valence bond (RVB) idea for the origin of high-T_c superconductivity quite seriously. The valence bonds are protected by the spin gap, and the effect of doping could well be to just turn the valence-bond solids into translational quantum liquids that transport two units of electrical charge. Focusing on the Berry phases in the pnictides one has only the options of an "intermediate" crystal-field $S=1$ state[10] or the high spin $S=2$ for the microscopic spin. In the former case the ground state has a twofold degeneracy and the building blocks are no longer pair singlets but instead the chain singlets. Thinking along the RVB lines, what to expect

when such a system is doped? The dopants will increase the quantum fluctuations but chains are not pairs. One anticipates that doping might drive the system into the nonmagnetic "Haldane chain phase" breaking the twofold rotational symmetry of the lattice. One notices that something of the kind is found in the phase diagram of the pnictides: the structural transition to the orthorombic phase persists to much higher dopings than the stripe antiferromagnetism.[49] At first view this seems rather detached from the RVB idea. But now one has to realize that the charge carriers are themselves spinful, carrying by default a half-integer spin. Taking for instance the intermediate $S=1$ background, the holes would carry $S=1/2$, and t-J models corresponding with a mix of $S=1$ and $S=1/2$ states have been studied in the past.[50] One anticipates that in an incompressible "chainlike" $S=1$ background the $S=1/2$ carriers might again be "glued by Berry forces" into valence-bond pairs, re-establishing a connection with the RVB mechanism of the cuprates. A similar idea has been previously proposed from a different approach.[51]

In conclusion, it is quite questionable that any of these considerations have a bearing on pnictide superconductivity but they do make the case that there is still much interesting physics to be explored dealing with systems characterized by a larger microscopic spin.

ACKNOWLEDGMENTS

We are grateful for stimulating discussion with M. Q. Weng. This work was partially supported by NSFC and the National Program for Basic Research of MOST, China, the DARPA OLE program, the (U.S.) DOE under Grant No. DE-FG02-06ER46305, the NSF under Grant No. DMR-0605696, and the Stichting voor Fundamenteel Onderzoek der Materie (FOM).

[1] Y. Kamihara, T. Watanabe, M. Hirano, and H. Hosono, J. Am. Chem. Soc. **130**, 3296 (2008).
[2] H. Takahashi, K. Igawa, A. Kazunobu, and Y. Kamihara, Nature (London) **453**, 376 (2008).
[3] Z. A. Ren, J. Yang, W. Lu, W. Yi, G. C. Che, X. L. Dong, L. L. Sun, and Z. X. Zhao, Mater. Res. Innovations **12**, 105 (2008).
[4] X. H. Chen, T. Wu, G. Wu, R. H. Liu, H. Chen, and D. F. Fang, Nature (London) **453**, 761 (2008).
[5] G. F. Chen, Z. Li, D. Wu, G. Li, W. Z. Hu, J. Dong, P. Zheng, J. L. Luo, and N. L. Wang, Phys. Rev. Lett. **100**, 247002 (2008).
[6] C. de la Cruz, Q. Huang, J. W. Lynn, W. R. J. Li, J. L. Zarestky, H. A. Mook, G. F. Chen, J. L. Luo, N. L. Wang, and P. Dai, Nature (London) **453**, 899 (2008).
[7] D.-X. Yao and E. W. Carlson, Phys. Rev. B **78**, 052507 (2008).
[8] J. Zhao *et al.*, Phys. Rev. Lett. **101**, 167203 (2008).
[9] M. A. McGuire *et al.*, Phys. Rev. B **78**, 094517 (2008).
[10] F. Krüger, S. Kumar, J. Zaanen, and J. van den Brink, Phys. Rev. B **79**, 054504 (2009).
[11] C. Xu, M. Muller, and S. Sachdev, Phys. Rev. B **78**, 020501(R) (2008).
[12] C. Fang, H. Yao, W.-F. Tsai, J. P. Hu, and S. A. Kivelson, Phys. Rev. B **77**, 224509 (2008).
[13] P. Chandra and B. Doucot, Phys. Rev. B **38**, 9335 (1988).
[14] J. H. Xu and C. S. Ting, Phys. Rev. B **42**, 6861 (1990).
[15] I. G. Gochev, Phys. Rev. B **51**, 16421 (1995).
[16] F. Mila, D. Poilblanc, and C. Bruder, Phys. Rev. B **43**, 7891 (1991).
[17] F. Krüger and S. Scheidl, Europhys. Lett. **74**, 896 (2006).
[18] E. Dagotto and A. Moreo, Phys. Rev. Lett. **63**, 2148 (1989).
[19] H. J. Schulz and T. A. L. Ziman, Europhys. Lett. **18**, 355 (1992).
[20] H. J. Schulz, T. A. L. Ziman, and D. Poilblanc, J. Phys. I **6**, 675 (1996).
[21] P. Sindzingre, Phys. Rev. B **69**, 094418 (2004).
[22] L. Capriotti and S. Sorella, Phys. Rev. Lett. **84**, 3173 (2000).
[23] L. Capriotti, F. Becca, A. Parola, and S. Sorella, Phys. Rev. Lett. **87**, 097201 (2001).
[24] M. P. Gelfand, R. R. P. Singh, and D. A. Huse, Phys. Rev. B **40**, 10801 (1989).
[25] M. P. Gelfand, Phys. Rev. B **42**, 8206 (1990).
[26] R. R. P. Singh, Z. Weihong, C. J. Hamer, and J. Oitmaa, Phys. Rev. B **60**, 7278 (1999).
[27] O. P. Sushkov, J. Oitmaa, and Z. Weihong, Phys. Rev. B **63**, 104420 (2001).
[28] O. P. Sushkov, J. Oitmaa, and Z. Weihong, Phys. Rev. B **66**, 054401 (2002).
[29] R. F. Bishop, D. J. J. Farnell, and J. B. Parkinson, Phys. Rev. B **58**, 6394 (1998).
[30] N. Read and S. Sachdev, Phys. Rev. Lett. **62**, 1694 (1989).
[31] N. Read and S. Sachdev, Phys. Rev. B **42**, 4568 (1990).
[32] S. Sachdev, Nat. Phys. **4**, 173 (2008).
[33] R. F. Bishop, P. H. Y. Li, R. Darradi, and J. Richter, Europhys. Lett. **83**, 47004 (2008).
[34] S. Moukouri, Phys. Lett. A **352**, 256 (2006).
[35] E. S. Sorensen and I. Affleck, Phys. Rev. Lett. **71**, 1633 (1993).
[36] F. D. M. Haldane, Phys. Lett. **93A**, 464 (1983).
[37] F. D. M. Haldane, Phys. Rev. Lett. **50**, 1153 (1983).
[38] S. Todo, M. Matsumoto, C. Yasuda, and H. Takayama, Phys. Rev. B **64**, 224412 (2001).
[39] F. Anfuso and A. Rosch, Phys. Rev. B **76**, 085124 (2007).
[40] M. denNijs and K. Rommelse, Phys. Rev. B **40**, 4709 (1989).
[41] Y. J. Kim and R. J. Birgeneau, Phys. Rev. B **62**, 6378 (2000).
[42] M. Matsumoto, C. Yasuda, S. Todo, and H. Takayama, Phys. Rev. B **65**, 014407 (2001).
[43] F. Alet and E. S. Sorensen, Phys. Rev. B **65**, 092408 (2002).
[44] R. Zinke, J. Schulenburg, and J. Richter, Eur. Phys. J. B **61**, 147 (2008).
[45] Z. Cai, S. Chen, S. Kou, and Y. Wang, Phys. Rev. B **76**, 054443 (2007).
[46] S. R. White, Phys. Rev. Lett. **69**, 2863 (1992).
[47] M. Sato and M. Oshikawa, Phys. Rev. B **75**, 014404 (2007).
[48] O. A. Starykh and L. Balents, Phys. Rev. Lett. **93**, 127202 (2004).
[49] J. Zhao *et al.*, Nature Mater. **7**, 953 (2008).
[50] J. Zaanen, A. M. Oles, and P. Horsch, Phys. Rev. B **46**, 5798 (1992).
[51] G. Baskaran, arXiv:0804.1341 (unpublished).